ISSN: (Online) 2410-1516, (Print) 2413-3183

Erratum: Chromatic properties of astigmatic eyes

Authors:
Tanya Evans[1]
William F. Harris[1]

Affiliations:
[1]Department of Optometry, University of Johannesburg, South Africa

Corresponding author:
Tanya Evans,
tevans@uj.ac.za

Dates:
Published: 06 Dec. 2019

How to cite this article:
Evans T, Harris WF. Erratum: Chromatic properties of astigmatic eyes. Afr Vision Eye Health. 2019;78(1), a540. https://doi.org/10.4102/aveh.v78i1.540

In the author list of this article published earlier, Tanya Evans' ORCID was unintentionally misprinted as https://orcid.org/0000-0002-5503-0245. The correct ORCID for Tanya Evans is https://orcid.org/0000-0001-8307-2912. The publisher sincerely regrets this error and apologises for any inconvenience caused.

Note: DOI of original article published: https://doi.org/10.4102/aveh.v77i1.435

African Vision and Eye Health
ISSN: (Online) 2410-1516, (Print) 2413-3183

Chromatic properties of astigmatic eyes

Authors:
Tanya Evans[1]
William F. Harris[1]

Affiliations:
[1]Department of Optometry, University of Johannesburg, South Africa

Corresponding author:
Tanya Evans,
tevans@uj.ac.za

Dates:
Received: 31 Oct. 2017
Accepted: 02 Mar. 2018
Published: 31 July 2018

How to cite this article:
Evans T, Harris WF. Chromatic properties of astigmatic eyes. Afr Vision Eye Health. 2018;77(1), a435. https://doi.org/10.4102/aveh.v77i1.435

Background: Chromatic differences in power, refractive compensation, position and magnification have been described in the literature for Gaussian eyes.

Aim: This article explores these definitions and defines chromatic properties for eyes that have astigmatic and decentred or tilted elements.

Setting: Linear optics.

Methods: The optical model is linear optics and makes use of the ray transference **T**.

Results: Results are presented as either 2 × 2 matrices or 2 × 1 vectors. The dependence of the chromatic properties on the position of an object and the limiting aperture is explored and results are presented as independent of, or dependent on, object and aperture position. Apertures undergo both longitudinal and transverse shifts in position. The results are general and apertures may include pupils or pinholes, either surgically inserted inside the eye or held in front of the eye. Numerical examples are provided for Le Grand's four-surface eye and an arbitrary astigmatic heterocentric four-surface eye.

Conclusion: *Aperture-independent chromatic properties* include chromatic difference in power and refractive compensation, both given as 2 × 2 matrices. *Aperture-dependent chromatic properties* are all dependent on longitudinal shifts in the plane of the limiting aperture. In addition, chromatic difference in position and inclination depend on both object and transverse aperture position. Chromatic difference in image size or angular spread depends on object position and is independent of transverse aperture position. These four aperture-dependent chromatic properties are given as 2 × 1 vectors. Chromatic magnifications are independent of object and transverse aperture position and are given as 2 × 2 matrices.

Introduction

The purpose of this article is to define chromatic properties for an eye with astigmatic and heterocentric elements. In physiological optics, longitudinal chromatic aberration[1,2,3,4,5,6,7] is defined as chromatic difference in focus (either the chromatic difference in power or the chromatic difference in refractive compensation). Transverse chromatic aberration[1,2,3,6,7,8,9,10,11] is defined as either chromatic difference in position or chromatic difference in magnification. The definitions for transverse chromatic aberration depend on the position of the nodal point.[1,2,9,11]

We use these definitions as the basis for generalising to chromatic properties of eyes that may have astigmatic and decentred or tilted refractive elements. Like others,[1,2,3,8,11] we too find that the pupil plays an important role in transverse chromatic properties of the eye; however, we seek definitions that do not depend on the nodal point. Firstly, in an astigmatic eye, the nodal points expand into nodal structures,[12] much like a focal point with its two-line foci and a circle of least confusion across the interval of Sturm and, secondly, nodal points depend on the frequency of light.[13] Nodal points are, therefore, not good structures on which to base definitions.

In astigmatic systems, the images at the retina of a dichromatic object point may comprise elliptically shaped red and blue blur patches, even when the pupil is circular. The two blur patches may differ in size and shape and may be relatively rotated. We define two properties that are independent of object and pupil position. Chromatic properties that depend on the object and the pupil position are defined in terms of the position, size and orientation of the red and blue images on the retina, and the inclination of the chief rays subtending these images.

The results obtained are general. The chromatic properties that depend on the pupil position can be extended to any system that has an aperture. Because of this, the results can be applied to any system that includes a pinhole aperture such as the Kamra corneal pinhole inlay[14] and the IC-8 pinhole intra-ocular lens,[15] both made by AcuFocus, or the Xtrafocus 93L intra-ocular pinhole implant[16] made by Morcher. These pinhole surgeries are all indicated for presbyopia and the Xtrafocus is additionally indicated for irregular astigmatism.

Method

The method relies on linear optics, including the ray transference:

$$\mathbf{T} = \begin{pmatrix} \mathbf{A} & \mathbf{B} & \mathbf{e} \\ \mathbf{C} & \mathbf{D} & \boldsymbol{\pi} \\ \mathbf{o}^{\mathrm{T}} & \mathbf{o}^{\mathrm{T}} & 1 \end{pmatrix},$$

a 5 × 5 matrix,[17,18] where **A** the dilation, **B** the disjugacy, **C** the divergence and **D** the divarication are each 2 × 2 submatrices, **e** the transverse translation and $\boldsymbol{\pi}$ the deflection are each 2 × 1 submatrices. Together **A**, **B**, **C**, **D**, **e** and $\boldsymbol{\pi}$ are the six fundamental paraxial optical properties of a system.[17] The bottom row is trivial; **o** is a 2 × 1 null matrix and superscript T represents the matrix transpose. (A matrix is represented in bold and a scalar in italics, for example, **y** and *y*.) The elements of the system may be astigmatic (which affect **A**, **B**, **C** and **D**) and heterocentric (which affect **e** and $\boldsymbol{\pi}$). **A**, **D** and $\boldsymbol{\pi}$ are unitless; **B** and **e** are in units of length, for example, metres; and **C** is in units of inverse length, for example, dioptres. The transference completely defines the effect the system has on rays traversing it.[19]

The ray state is defined by the 5 × 1 matrix[17,18,20]

$$\boldsymbol{\gamma} = \begin{pmatrix} \mathbf{y} \\ \boldsymbol{\alpha} \\ 1 \end{pmatrix},$$

where **y** the transverse position and $\boldsymbol{\alpha}$ the reduced inclination, given by $\boldsymbol{\alpha} = n\mathbf{a}$, are both 2 × 1 submatrices and n is the refractive index of the surrounding medium.[20] **a** is the inclination. The ray state at incidence $\boldsymbol{\gamma}_0$ onto the system is changed to $\boldsymbol{\gamma}$ at emergence through the relationship[17,18]

$$\mathbf{T}\boldsymbol{\gamma}_0 = \boldsymbol{\gamma}.$$

The transference depends on the frequency of light[21,22] through the refractive indices of the media. Frequency is independent of the medium and provides expressions that are closer to being linear and therefore is preferable to vacuum wavelength.[22,23] We make use of formulae for the refractive indices of the media based on Le Grand's [24] eye given by Villegas et al.[25] to obtain frequency-dependent transferences and reduced inclination.

Power $\mathbf{F} = -\mathbf{C}$ and corneal-plane refractive compensation $\mathbf{F}_0 = \mathbf{B}^{-1}\mathbf{A}$, both 2 × 2 matrices, are obtained from **T**.[17] Chromatic difference in power[22] is defined as $\delta\mathbf{F} = \mathbf{F}^{\mathrm{b}} - \mathbf{F}^{\mathrm{r}}$ where superscripts b and r represent two frequencies. For convenience, we shall call them blue and red. Other chromatic differences are defined similarly; they are obtained from transferences corresponding to the red and blue frequencies. The chromatic difference in refractive compensation[22] is $\delta\mathbf{F}_0 = \mathbf{F}_0^{\mathrm{b}} - \mathbf{F}_0^{\mathrm{r}}$. These two chromatic properties depend on neither object position nor limiting aperture and we refer to them as *aperture-independent chromatic properties*. Examples are provided in Table 1.

Harris[17] describes the magnification, blur and ray state at the retina for an astigmatic heterocentric eye. The eye naturally partitions into anterior and posterior portions at the plane of the pupil, a limiting aperture. If a pinhole is surgically implanted in the eye, then it partitions the eye into anterior and posterior subsystems at the plane of the pinhole. In this situation, we make the reasonable assumption that the pinhole is the limiting aperture. The anterior subsystem has transference $\mathbf{T}_{\mathrm{A}}$ and the posterior subsystem $\mathbf{T}_{\mathrm{B}}$. Hence, the eye has transference[17,18] $\mathbf{T}_{\mathrm{E}} = \mathbf{T}_{\mathrm{B}}\mathbf{T}_{\mathrm{A}}$. Subscripts A, B and E are used to represent the anterior and posterior subsystems and the system of the eye, respectively.

To define chromatic differences at the retina, we are interested not in reduced inclination $\boldsymbol{\alpha}$ but in (unreduced) inclination **a** of rays. Accordingly, we adjust and summarise Harris's[17] results to obtain the coefficient matrix:

$$\mathbf{V}_{\mathrm{E}} = \begin{pmatrix} \mathbf{W}_{\mathrm{E}} & \mathbf{X}_{\mathrm{E}} & \mathbf{g}_{\mathrm{E}} \\ \mathbf{Y}_{\mathrm{E}} & \mathbf{Z}_{\mathrm{E}} & \mathbf{h}_{\mathrm{E}} \\ \mathbf{o}^{\mathrm{T}} & \mathbf{o}^{\mathrm{T}} & 1 \end{pmatrix} = \begin{pmatrix} \mathbf{A}_{\mathrm{E}}\mathbf{A}_{\mathrm{A}}^{-1} & n_0\mathbf{B}_{\mathrm{B}}\mathbf{A}_{\mathrm{A}}^{-\mathrm{T}} & \mathbf{B}_{\mathrm{B}}\mathbf{C}_{\mathrm{A}}\mathbf{A}_{\mathrm{A}}^{-1}\mathbf{e}_{\mathrm{A}} + \mathbf{B}_{\mathrm{B}}\boldsymbol{\pi}_{\mathrm{A}} + \mathbf{e}_{\mathrm{B}} \\ n^{-1}\mathbf{C}_{\mathrm{E}}\mathbf{A}_{\mathrm{A}}^{-1} & n_0 n^{-1}\mathbf{D}_{\mathrm{B}}\mathbf{A}_{\mathrm{A}}^{-\mathrm{T}} & n^{-1}\left(\mathbf{D}_{\mathrm{B}}\mathbf{C}_{\mathrm{A}}\mathbf{A}_{\mathrm{A}}^{-1}\mathbf{e}_{\mathrm{A}} + \mathbf{D}_{\mathrm{B}}\boldsymbol{\pi}_{\mathrm{A}} + \boldsymbol{\pi}_{\mathrm{B}}\right) \\ \mathbf{o}^{\mathrm{T}} & \mathbf{o}^{\mathrm{T}} & 1 \end{pmatrix},$$

[Eqn 1]

a 5 × 5 matrix with the same block-matrix structure and units as the transference. $\mathbf{W}_{\mathrm{E}}$ is the distance image blur coefficient, $\mathbf{X}_{\mathrm{E}}$ is the distance image size coefficient, $\mathbf{g}_{\mathrm{E}}$ is the distance image displacement, $\mathbf{Y}_{\mathrm{E}}$ is the directional spread coefficient, $\mathbf{Z}_{\mathrm{E}}$ is the distant directional coefficient and $\mathbf{h}_{\mathrm{E}}$ is the distant directional displacement.[17] Each of the coefficients is made up of the fundamental properties of the eye and the anterior and posterior subsystems. Light from a distant object arrives at the cornea with inclination $\mathbf{a}_{\mathrm{K}}$, traverses the pupil or pinhole with position $\mathbf{y}_{\mathrm{P}}$ and reaches the retina with transverse position $\mathbf{y}_{\mathrm{R}}$ and inclination $\mathbf{a}_{\mathrm{R}}$. We define modified ray state $\mathbf{r}_{\mathrm{R}} = \begin{pmatrix} \mathbf{y}_{\mathrm{R}}^{\mathrm{T}} & \mathbf{a}_{\mathrm{R}}^{\mathrm{T}} & 1 \end{pmatrix}^{\mathrm{T}}$. Then $\mathbf{V}_{\mathrm{E}}\mathbf{v} = \mathbf{r}_{\mathrm{R}}$ where $\mathbf{v} = \begin{pmatrix} \mathbf{y}_{\mathrm{P}}^{\mathrm{T}} & \mathbf{a}_{\mathrm{K}}^{\mathrm{T}} & 1 \end{pmatrix}^{\mathrm{T}}$. Like the transference, $\mathbf{V}_{\mathrm{E}}$ depends on the frequency of light.

We define chromatic difference in image position $\delta\mathbf{y}_{\mathrm{R}}$ as the position of the blue relative to the red retinal image and

TABLE 1: Aperture-independent chromatic properties.

Properties	Le Grand's eye	Astigmatic heterocentric model eye
Chromatic difference in power	δF = 2.5158 D	$\delta\mathbf{F} = \begin{pmatrix} 2.8649 & 0.0552 \\ 0.0468 & 2.6004 \end{pmatrix}\mathrm{D} \approx 2.8743\{9.7^\circ\}\ 2.5910\{101.4^\circ\}$
Chromatic difference in refractive compensation	δF_0 = −1.9013 D	$\delta\mathbf{F}_0 = \begin{pmatrix} -2.3160 & -0.0596 \\ -0.0596 & -1.9833 \end{pmatrix}\mathrm{D} \approx -2.3264\{9.9^\circ\} - 1.9729\{99.9^\circ\}$

Note: The eigenstructure is provided for ease of interpretation (given as each eigenvalue or power along its corresponding eigenmeridian in degrees).

chromatic difference in inclination of the chief rays at the retina $\delta\mathbf{a}_R$, as shown in Figure 1. These are summarised as the chromatic difference in physical ray states at the retina $\delta\mathbf{r}_R = \left(\delta\mathbf{y}_R^T \quad \delta\mathbf{a}_R^T \quad 0\right)^T$. Substituting from Equation 1, we obtain $\delta\mathbf{V}_E\,\mathbf{v} = \delta\mathbf{r}_R$ or

$$\begin{pmatrix} \delta\mathbf{W}_E & \delta\mathbf{X}_E & \delta\mathbf{g}_E \\ \delta\mathbf{Y}_E & \delta\mathbf{Z}_E & \delta\mathbf{h}_E \\ \mathbf{o}^T & \mathbf{o}^T & 0 \end{pmatrix}\begin{pmatrix} \mathbf{y}_P \\ \mathbf{a}_K \\ 1 \end{pmatrix} = \begin{pmatrix} \delta\mathbf{y}_R \\ \delta\mathbf{a}_R \\ 0 \end{pmatrix}, \qquad \text{[Eqn 2]}$$

where $\delta\mathbf{V}_E = \mathbf{V}_E^b - \mathbf{V}_E^r$ is the chromatic difference in coefficient matrices. Examples are provided in Table 2. By definition,[1,2,3,9,10] we are following the chief ray and by implication ignoring blur and the size of the aperture. All chromatic differences are defined as from red to blue, that is, from a low to a high frequency and energy.

When a pinhole is placed in front of the eye, the anterior transference becomes an identity matrix and Equation 2 simplifies. In this situation, only $\delta\mathbf{X}_E$ and $\delta\mathbf{Z}_E$ are dependent on z, the position of the pinhole in front of the eye. An example is provided in Table 2c. A pinhole placed in front of the eye holds more interest for clinical and experimental settings; some phenomena are exaggerated and, so, may lead to more insight.

$\Delta\mathbf{a}_K$ is the angular spread subtended by the two extreme points of a distant object. Red and blue images of sizes $\Delta\mathbf{y}_R^r$ and $\Delta\mathbf{y}_R^b$ are formed on the retina. We use δ to represent a chromatic difference and Δ to represent size or angular spread between rays of the same frequency. The chromatic difference in image size at the retina is $\delta(\Delta\mathbf{y}_R)$. Similarly, $\delta(\Delta\mathbf{a}_R)$ is the difference in angular spread between the red and blue chief rays arriving at the retina. $\delta(\Delta\mathbf{y}_R)$ and $\delta(\Delta\mathbf{a}_R)$ are both linear in $\Delta\mathbf{a}_K$. We obtain the summary $\delta\mathbf{V}_E\Delta\mathbf{v} = \delta(\Delta\mathbf{r}_R)$ where $\Delta\mathbf{y}_P = \mathbf{o}$, ignoring any blur component. Consequently, aperture size and shape are irrelevant. Hence,

$$\begin{pmatrix} \bullet & \delta\mathbf{X}_E & \bullet \\ \bullet & \delta\mathbf{Z}_E & \bullet \\ \mathbf{o}^T & \mathbf{o}^T & 0 \end{pmatrix}\begin{pmatrix} \mathbf{o} \\ \Delta\mathbf{a}_K \\ 0 \end{pmatrix} = \begin{pmatrix} \delta(\Delta\mathbf{y}_R) \\ \delta(\Delta\mathbf{a}_R) \\ 0 \end{pmatrix}, \qquad \text{[Eqn 3]}$$

where $\bullet$ represents entries that are nullified. This is illustrated in Figure 2. $\delta(\Delta\mathbf{y}_R)$ and $\delta(\Delta\mathbf{a}_R)$ are independent of the transverse position of the aperture $\mathbf{y}_p$ but are dependent on the longitudinal position of the aperture (which are contained in $\delta\mathbf{X}_E$ and $\delta\mathbf{Z}_E$) and the object's angular size $\Delta\mathbf{a}_K$.

We define chromatic image size magnification $\mathbf{M}_{yR}$ by means of $\mathbf{M}_{yR}\Delta\mathbf{y}_R^r = \Delta\mathbf{y}_R^b$. From Equation 3 and manipulating we obtain

$$\mathbf{M}_{yR} = \mathbf{X}_E^b\mathbf{X}_E^{r-1}. \qquad \text{[Eqn 4]}$$

$\Delta\mathbf{y}_R^r$ and $\Delta\mathbf{y}_R^b$ are shown in Figure 2. Similarly, we define the retinal chromatic angular spread magnification as $\mathbf{M}_{aR}\Delta\mathbf{a}_R^r = \Delta\mathbf{a}_R^b$. Hence,

$$\mathbf{M}_{aR} = \mathbf{Z}_E^b\mathbf{Z}_E^{r-1}. \qquad \text{[Eqn 5]}$$

$\mathbf{M}_{yR}$ and $\mathbf{M}_{aR}$ are 2 × 2 magnification matrices whose eigenstructure reveals the magnitude and direction of minimum and maximum magnification. Examples are given in Table 3.

Results – numerical examples

For a Gaussian eye, such as a model eye, all the results reduce to scalars. We present numerical examples for two eyes;

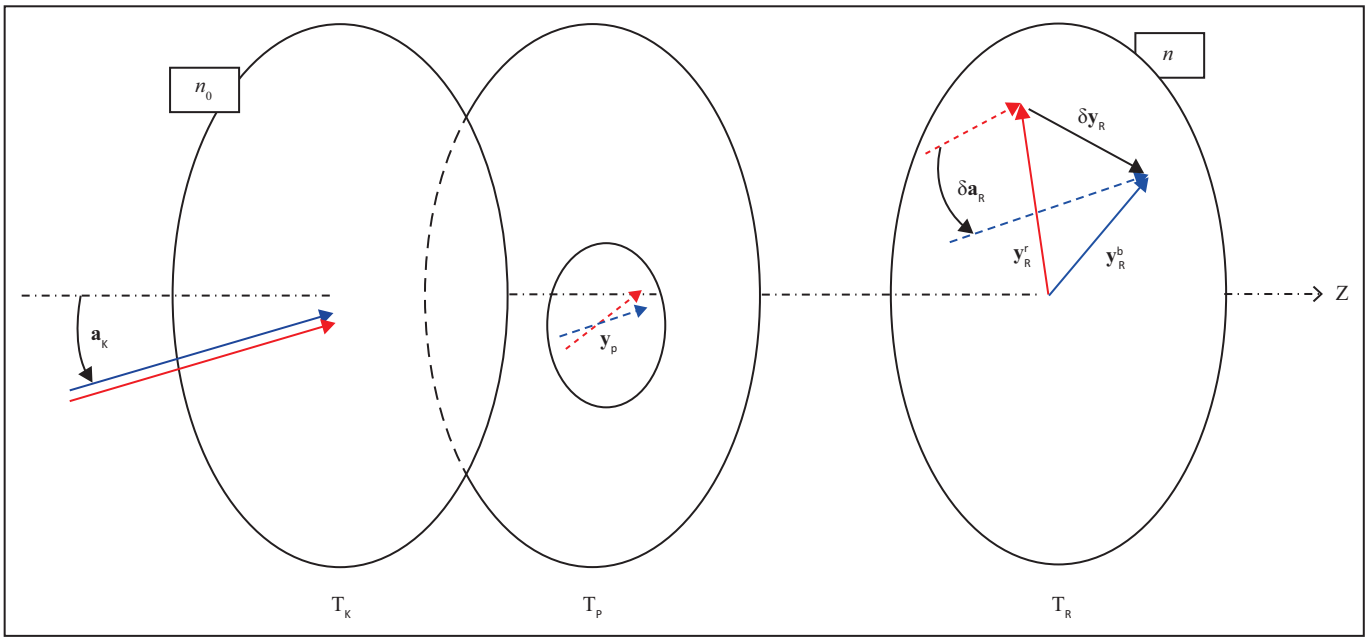

FIGURE 1: A general eye with corneal T_K, pupillary T_P and retinal transverse planes T_R. A pencil of rays enters the eye at T_K from a distant object with inclination $\mathbf{a}_K$ and we select only the red and blue chief rays traversing the centre of the (decentred) pupil $\mathbf{y}_p$ at T_P. The chromatic difference in image position $\delta\mathbf{y}_R$ is the vector from the position of the red ray $\mathbf{y}_R^r$ to the blue ray $\mathbf{y}_R^b$ at the plane of the retina T_R. Similarly, the chromatic difference in inclination of the chief rays at the retina $\delta\mathbf{a}_R$ is measured from the red ray $\mathbf{a}_R^r$ to the blue ray $\mathbf{a}_R^b$. All ray positions, inclinations and pupil decentration are exaggerated for clarity.

TABLE 2: Chromatic properties dependent on object ($\mathbf{a}_K$) and aperture ($\mathbf{y}_P$) position (Equation 2).

Eye	Chromatic properties
a Le Grand's naked eye	$\begin{pmatrix} -0.0357 & -0.1258\times10^{-3}\ \text{m} \\ -1.8220\ \text{D} & -6.011\times10^{-3} \end{pmatrix}\begin{pmatrix} y_P \\ a_K \end{pmatrix}=\begin{pmatrix} \delta y_R \\ \delta a_R \end{pmatrix}$
b Pinhole in front of eye as function of distance z in front of eye	$\begin{pmatrix} -0.0315 & -0.0315(z)-0.2212\ \text{m} \\ -1.4143\ \text{D} & -1.4143\ \text{D}(z)-0.0033 \end{pmatrix}\begin{pmatrix} y_P \\ a_K \end{pmatrix}=\begin{pmatrix} \delta y_R \\ \delta a_R \end{pmatrix}$
c Kamra corneal pinhole inlay	$\begin{pmatrix} -0.0317 & -0.2166\times10^{-3}\ \text{m} \\ -1.4339\ \text{D} & -0.0092 \end{pmatrix}\begin{pmatrix} y_P \\ a_K \end{pmatrix}=\begin{pmatrix} \delta y_R \\ \delta a_R \end{pmatrix}$
d A naked astigmatic heterocentric model eye	$\begin{pmatrix} -0.0426 & -0.0006 & -0.1134\times10^{-3}\ \text{m} & -0.0021\times10^{-3}\ \text{m} & -0.0130\times10^{-3}\ \text{m} \\ -0.0005 & -0.0359 & -0.0023\times10^{-3}\ \text{m} & -0.1332\times10^{-3}\ \text{m} & 0.0064\times10^{-3}\ \text{m} \\ -2.1716\ \text{D} & -0.0372\ \text{D} & -0.0054 & -0.0001 & -0.0007 \\ -0.0330\ \text{D} & -1.8562\ \text{D} & -0.0001 & -0.0065 & 0.0003 \\ 0 & 0 & 0 & 0 & 0 \end{pmatrix}\begin{pmatrix} \mathbf{y}_P \\ \mathbf{a}_K \\ 1 \end{pmatrix}=\begin{pmatrix} \delta\mathbf{y}_R \\ \delta\mathbf{a}_R \\ 0 \end{pmatrix}$

a, Le Grand's eye with pupil as aperture; b, Le Grand's eye with handheld pinhole in front as a function of z ($\delta\mathbf{V}_P(z)$) with z measured from the cornea; c, Le Grand's eye with Kamra corneal pinhole inlay; d, an arbitrary astigmatic heterocentric model eye with pupil as aperture.

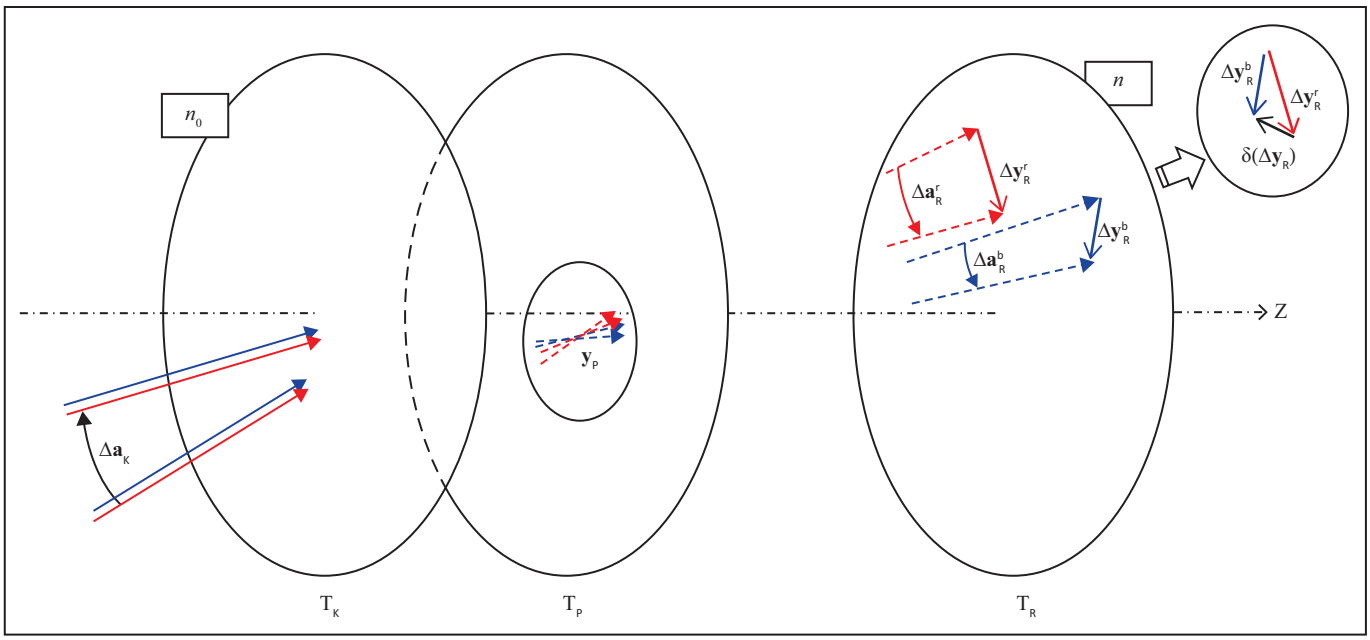

FIGURE 2: A general eye with corneal T_K, pupillary T_P and retinal transverse planes T_R. A pencil of rays enters the eye at T_K from a distant object with angular size $\Delta\mathbf{a}_K$. We trace only the red and blue rays traversing the same position in the pupil $\mathbf{y}_P$ in T_P. The chromatic difference in image size $\delta(\Delta\mathbf{y}_R)$ is the vector from the position of the red image of size $\Delta\mathbf{y}^r_R$ to the blue image of size $\Delta\mathbf{y}^b_R$ in T_R and shown in the inset. Similarly, the chromatic difference in angular spread at the retina is $\delta(\Delta\mathbf{a}_R)$. All ray positions, inclinations, object and image sizes, and pupil decentration are exaggerated for clarity.

TABLE 3: Chromatic magnification.

Variable	Chromatic image size magnification	Chromatic angular spread magnification
a	$M_{yR}=0.9925\ (\approx -0.75\ \%)$	$M_{aR}=0.9926\ (\approx -0.74\%)$
b	$M_{yR}=0.9870\ (\approx -1.3\%)$	$M_{aR}=0.9865\ (\sim -1.35\%)$
c	$\boldsymbol{M}_{yR}=\begin{pmatrix} 0.9933 & -0.1672\times10^{-3} \\ -0.1778\times10^{-3} & 0.9919 \end{pmatrix}$ $0.9934\{173.2°\}0.9918\{83.6°\}$ $\approx -0.66\%\{173.2°\}-0.82\%\{83.6°\}$	$\boldsymbol{M}_{aR}=\begin{pmatrix} 0.9935 & -0.2048\times10^{-3} \\ -0.2177\times10^{-3} & 0.9919 \end{pmatrix}$ $0.9935\{172.26°\}0.9919\{82.71°\}$ $\approx -0.65\%\{172.26°\}-0.81\%\{82.71°\}$

Note: (Equations 4 and 5) for a, Le Grand's eye with aperture at pupillary plane; b, Le Grand's eye with Kamra corneal inlay; c, an astigmatic heterocentric eye with aperture at pupillary plane; the eigenstructure is given for ease of interpretation.

Le Grand's four-surface eye[24] and an arbitrary four-surface astigmatic heterocentric eye for a chromatic difference from 430 THz to 750 THz (vacuum wavelengths 697.2 nm and 399.7 nm). The parameters of this eye are provided in an appendix for the two frequencies, along with the transferences and coefficient matrices for the red and blue frequencies. The aperture-independent properties are given in Table 1. Le Grand's eye [24] is emmetropic at a reference frequency of

509 THz (vacuum wavelength 589.0 nm) and the magnitude δF_0 is as expected.[1,4,8,26,27]

For the astigmatic eye $\delta\mathbf{F}$ may be an asymmetric matrix with non-orthogonal principal meridians. The results highlight the fact that the eye's power and refractive compensation are not simply related. $\delta\mathbf{F}$ and $\delta\mathbf{F}_0$ both yield astigmatic results; hence, the aperture-independent chromatic properties vary with the ametropia of the eye.

The chromatic properties dependent on object and aperture position are given in Table 2 and Table 3. The chromatic differences in position and inclination are given for Le Grand's eye for three different aperture positions in Table 2a to Table 2c. Included are examples with the Kamra corneal pinhole inlay,[14] implanted at a depth of 200 μm into the stroma and a pinhole held in front of the eye. Handheld pinholes and Kamra corneal inlays are more susceptible to transverse displacement than the natural pupil, which in turn affects δy_R and δa_R. When a_K = 5°, δy_R is zero at a position of y_P = –0.60 mm and δa_R is zero at y_P = –0.56 mm which represents nasal displacement in the left eye. This agrees approximately with the findings of Tabernero and Artal.[28] (They used wavelengths of 470 nm, 510 nm, 550 nm, 610 nm and 650 nm. Results will depend on the individual eye, the value used for angle κ and the formulae used for the wavelength-dependent refractive indices.) A comparison of Table 2a and Table 2c shows that δX_E and δZ_E increase in magnitude as the aperture plane moves anterior in Le Grand's eye. Hence, once a corneal inlay is positioned, off-axial object points increase the magnitude of δy_R and δa_R.

The results given in Table 2d for $\delta\mathbf{V}_E$ show that each of $\delta\mathbf{W}_E$, $\delta\mathbf{X}_E$, $\delta\mathbf{Y}_E$ and $\delta\mathbf{Z}_E$ are asymmetric. All of the coefficient matrices given in Table 2 can be applied to Equation 3 to obtain the $\delta(\Delta\mathbf{y}_R)$ and $\delta(\Delta\mathbf{a}_R)$. From the asymmetric entries of $\delta\mathbf{V}_E$ in Table 2d, we conclude that the red and blue images of size $\Delta\mathbf{y}_R^r$ and $\Delta\mathbf{y}_R^b$ may differ not only in size, but also in orientation.

Table 3a gives the chromatic magnifications that compare favourably with experimental results for chromatic difference in magnification.[1,6,11] In Table 3b, M_{yR} and M_{aR} increase as the plane of the limiting aperture is moved to the corneal-plane, as in the case of a Kamra corneal inlay. The values in Table 3c show that chromatic magnification in an astigmatic eye may differ along different meridians. The unequal diagonal entries and non-null off-diagonal entries imply that the chromatic magnification is not equal in all directions. The eigenstructure illustrates how the red and blue images are magnified by maximum and minimum amounts. The asymmetry of the chromatic magnification matrices indicates that the red and blue images are rotated with respect to each other. This is confirmed by the non-orthogonal eigenvectors. Although the misalignment of the eigenmeridians is small, this gives us insight into the effect of astigmatism.

Discussion

Traditional definitions for chromatic difference in focus, position and magnification are extended here to include eyes that have astigmatic and decentred or tilted refracting elements. We consistently use differences from red to blue (from low to high frequency and energy) and to avoid definitions that depend on nodal points because these are frequency-dependent in real eyes and not necessarily points in the presence of astigmatism.

Definitions for transverse chromatic aberration in the literature[1,2,3, 8,9,10,11] depend on the position of the rays reaching the retina. Angular measurements are taken from the nodal point and are not true ray inclinations. Within the limitations of first-order optics, we have used actual ray inclinations. The results for the illustrated astigmatic eye highlight the fact that chromatic properties are dependent on the ametropia of the eye.

Two aperture-independent chromatic properties are defined for eyes that include astigmatic elements, namely chromatic difference in power $\delta\mathbf{F}$ and refractive compensation $\delta\mathbf{F}_0$. These depend, among other things, on the ametropia of the eye and $\delta\mathbf{F}$ may be asymmetric. In an astigmatic eye, $\delta\mathbf{F}$ and $\delta\mathbf{F}_0$ may both be astigmatic powers. The principal meridians may be non-orthogonal for chromatic difference in power because the eye is a thick-lens system.

The aperture-dependent chromatic properties are all dependent on the longitudinal position of the aperture. In addition, chromatic difference in image position $\delta\mathbf{y}_R$ and inclination $\delta\mathbf{a}_R$ at the retina depend on $\mathbf{y}_P$ and $\mathbf{a}_K$. The positional differences between the red and blue rays are not limited to the Gaussian plane but are given as vectors across the transverse plane of the retina. Similarly, the inclinational differences represent the difference in inclination from red to blue chief rays and do not depend on the position of the nodal point or nodal structure. A transverse shift in aperture position $\mathbf{y}_P$, such as a misaligned corneal inlay or pinhole, will affect $\delta\mathbf{y}_R$ and $\delta\mathbf{a}_R$. This has importance for surgically inserted apertures, particularly corneal pinhole inlays which are sensitive to misalignment.[28]

The chromatic difference in image size $\delta(\Delta\mathbf{y}_R)$ and angular spread $\delta(\Delta\mathbf{a}_R)$ at the retina are independent of $\mathbf{y}_P$, but are dependent on the size of the object $\Delta\mathbf{a}_K$. The relationships are linear in $\Delta\mathbf{a}_K$. The red and blue images at the retina may differ both in size and orientation, represented by the vectorial difference. A shift in longitudinal position of the aperture, for example, from the iridial plane to the corneal-plane, increases the magnitude and exaggerates any relative rotation of red and blue images. However, of greater significance is chromatic magnification.

Chromatic magnification is a generalised ratio of the blue to red image size $\mathbf{M}_{yR}$ and angular spread $\mathbf{M}_{aR}$. Chromatic magnification is independent of $\mathbf{a}_K$ and $\mathbf{y}_P$, but is dependent on the longitudinal position of the limiting aperture. The chromatic magnification matrices show that the red and blue images undergo unequal magnification in the two principal meridians and that the red and blue images are rotated with respect to each other. (A scalar matrix implies equal chromatic magnification in all meridians. Unequal

diagonal and non-zero off-diagonal entries imply unequal magnification along principal meridians. Unequal off-diagonal entries show that the images are rotated.)

The aperture-independent chromatic properties $\delta\mathbf{F}$ and $\delta\mathbf{F}_0$ are obtained directly from the red and blue transferences $\mathbf{T}_E$. The aperture-dependent chromatic properties are all interrelated through the red and blue coefficient matrices $\mathbf{V}_E$ (Equation 1). Chromatic magnification is obtained from the entries of $\mathbf{V}_E$. Subtracting the red from the blue coefficient matrices gives us the chromatic difference of coefficient matrices $\delta\mathbf{V}_E$, from which we obtain the chromatic difference in position, inclination, image size and angular spread. The relationships of the entries of $\delta\mathbf{V}_E$ with aperture position and object position or size are given by Equations 2 and 3. Through $\mathbf{T}_E$ and $\mathbf{V}_E$ for red and blue light we obtain simple relationships among the chromatic properties of the eye.

The introduction of surgically implanted pinholes creates new interest in the effects of aperture-dependent chromatic properties. The corneal inlay increases the magnitude of chromatic magnification because of its longitudinal positioning and is sensitive to misalignment. The Xtrafocus 93L is intended for treating irregular astigmatism, so the chromatic effects of such a system in an astigmatic eye need to be known.

The values obtained for each of the aperture-dependent chromatic properties are small. However, these results give insight not only into the chromatic properties of the eye and the influence of limiting apertures, but also into the effect of astigmatism.

Acknowledgements

The authors would like to express their appreciation for the support from the National Research Foundation of South Africa. This article was presented as a poster at the conference Visual and Physiological Optics 2016, held in Antwerp, Belgium.

Competing interests

The authors declare that they have no financial or personal relationships that may have inappropriately influenced them in writing this article.

Authors' contributions

This work is based on research performed by TE towards a higher degree under the guidance of WFH.

References

1. Thibos LN, Bradley A, Zhang X. Effect of ocular chromatic aberration on monocular visual performance. Optom Vis Sci. 1991;68:599–607. https://doi.org/10.1097/00006324-199108000-00005
2. Thibos LN, Bradley A, Still DL, Zhang X, Howarth PA. Theory and measurement of ocular chromatic aberration. Vis Res. 1990;30:33–49. https://doi.org/10.1016/0042-6989(90)90126-6
3. Zhang X, Bradley A, Thibos LN. Experimental determination of the chromatic difference of magnification of the human eye and the location of the anterior nodal point. J Opt Soc Am A. 1993;10:213–220. https://doi.org/10.1364/JOSAA.10.000213
4. Wald G, Griffin DR. The change in refractive power of the human eye in dim and bright light. J Opt Soc Am. 1947;37:321–336. https://doi.org/10.1364/JOSA.37.000321
5. Cooper DP, Pease PL. Longitudinal chromatic aberration of the human eye and wavelength in focus. Am J Optom Physiol Opt. 1988;65:99–107. https://doi.org/10.1097/00006324-198802000-00006
6. Rabbetts RB. Bennett & Rabbetts' clinical visual optics. 4th ed. London: Butterworth-Heinemann-Elsevier, 2007; p. 287–293.
7. Atchison DA, Smith G. Optics of the eye. London: Butterworth-Heinemann, 2000; p. 180–192.
8. Thibos LN, Ye M, Zhang X, Bradley A. The chromatic eye: A new reduced-eye model of ocular chromatic aberration in humans. Appl Opt. 1992;31:3594–3600. https://doi.org/10.1364/AO.31.003594
9. Thibos LN. Calculation of the influence of lateral chromatic aberration on image quality across the visual field. J Opt Soc Am. 1987;4:1673–1680. https://doi.org/10.1364/JOSAA.4.001673
10. Simonet P, Campbell MCW. The optical transverse chromatic aberration on the fovea of the human eye. Vis Res. 1990;30:187–206. https://doi.org/10.1016/0042-6989(90)90035-J
11. Zhang X, Thibos LN, Bradley A. Relation between the chromatic difference of refraction and the chromatic difference of magnification for the reduced eye. Optom Vis Sci. 1991;68:456–458. https://doi.org/10.1097/00006324-199106000-00007
12. Harris WF. Cardinal points and generalizations. Ophthal Physiol Opt. 2010;30:391–401. https://doi.org/10.1111/j.1475-1313.2010.00760.x
13. Evans T, Harris WF. Cardinal and anti-cardinal points, equalities and chromatic dependence. Ophthal Physiol Opt. 2017;37:353–357.
14. Acufocus. The Kamra inlay. Doctor Sales Pamphlet. p. 1–5. [cited 2017 Sept 18]. Available from http://www.acufocus.com/int/sites/default/files/MK-1253%20Rev%20C%2C%20KAMRA%20Doctor%20Sales%20Pamphlet%20PAGE-BY-PAGE.pdf
15. Acufocus. IC-8 Small aperture IOL. Physician Brochure. p. 1–7. [cited 2017 Sept 18]. Available from http://www.acufocus.com/int/sites/default/files/MK-1268%20Rev%20A%2C%20IC-8%20IOL%20Physician%20Brochure.pdf
16. Morcher Ophthalmic Implants. Special implants: Xtrafocus intraocular implant. [cited 2017 Sept 23]. Available from: http://www.morcher.com/nc/en/products/special-implants.html
17. Harris WF. Magnification, blur, and ray state at the retina for the general eye with and without a general optical instrument in front of it: 1. Distant objects. Optom Vis Sci. 2001;78:888–900. https://doi.org/10.1097/00006324-200112000-00011
18. Harris WF. Paraxial ray tracing through noncoaxial astigmatic optical system, and a 5 × 5 augmented system matrix. Optom Vis Sci. 1994;71:282–285. https://doi.org/10.1097/00006324-199404000-00009
19. Torre A. Linear ray and wave optics in phase space. Amsterdam: Elsevier, 2005; p. 60.
20. Harris WF. Realizability of optical systems of given linear optical character. Optom Vis Sci. 2004;81:807–809. https://doi.org/10.1097/00006324-200410000-00014
21. Evans T, Harris WF. Dependence of the ray transference of model eyes on the frequency of light. Afr Vision Eye Health. 2016;75:a322. https://doi.org/10.4102/aveh.v75i1.322
22. Evans T, Harris WF. Dependence of the transference of a reduced eye on frequency of light. S Afr Optom. 2011;70:149–155. https://doi.org/10.4102/aveh.v70i4.112
23. Pease PL, Barbeito R. Axial chromatic aberration of the human eye: Frequency or wavelength? Ophthal Physiol Opt. 1989;9:215–217.
24. Le Grand Y. Optique Physiologique. Tome Premier, le Dioptrique de l'Œil et sa Correction. Paris: Revue d'Optique, 1945; p. 50–51.
25. Villegas ER, Carretero L, Fimia A. Le Grand eye for the study of ocular chromatic aberration. Ophthal Physiol Opt. 1996;16:528–531. https://doi.org/10.1016/0275-5408(96)00007-5
26. Atchison DA, Smith G, Waterworth MD. Theoretical effect of refractive error and accommodation on longitudinal chromatic aberration of the human eye. Optom Vis Sci. 1993;70:716–722. https://doi.org/10.1097/00006324-199309000-00006
27. Howarth PA, Bradley A. The longitudinal chromatic aberration of the human eye, and its correction. Vis Res. 1986;26:361–366. https://doi.org/10.1016/0042-6989(86)90034-9
28. Tabernero J, Artal P. Optical modelling of a corneal inlay in real eyes to increase depth of focus: Optimum centration and residual defocus. J Cataract Refract Surg. 2012;38:270–277. https://doi.org/10.1016/j.jcrs.2011.07.040

Appendix starts on the next page →

Appendix 1

The results given in Table 2d and Table 3c are based on an arbitrary four-surface astigmatic heterocentric eye. The parameters of this eye are given in Table 1-A1. The parameters were introduced previously,[1] however, different frequencies have been chosen for this example. K1 and K2 are the first and second surfaces of the cornea, while L1 and L2 are the first and second surfaces of the crystalline lens. The tilt is given as horizontal and vertical components in radians. For K1, the right side of the cornea will be tilted away from and the top towards an observer looking at the eye. Villegas, Carretero and Fimia[2] published equations for the four media of Le Grand's eye and we apply these here. The media are given as cornea (K), aqueous humour (A), lens (L) and vitreous humour (V). Refractive indices for the four media for frequencies of 430 THz and 750 THz are given in Table 1-A1.

TABLE 1-A1: Principal radii of curvature and tilts of the four surfaces and separations and refractive indices of the four media of the arbitrary astigmatic heterocentric eye used in the numerical example.

Variable	Principal radii (mm{deg}mm)	Tilt (radians)	Separation (mm)	Refractive index for 430 THz (red)	Refractive index for 750 THz (blue)
K1	6.5{180}8	$(0.06\ \ -0.05)^T$	-	-	-
K	-	-	0.5	1.3729	1.3883
K2	5.8{20}7.2	$(0.04\ \ 0.06)^T$	-	-	-
A	-	-	3.0	1.3325	1.3474
L1	10.2{100}8.7	$(-0.07\ \ 0.1)^T$	-	-	-
L	-		4.0	1.4161	1.4339
L2	–4.5{70}–6.5	$(-0.05\ \ -0.03)^T$	-	-	-
V	-	-	16.5	1.3327	1.3464

The transferences for red and blue light are:

$$\mathbf{T}_r=\begin{pmatrix} -0.1487 & -0.0133 & 16.5836\times10^{-3}\ \text{m} & -0.1291\times10^{-3}\ \text{m} & -0.3123\times10^{-3}\ \text{m} \\ -0.0121 & -0.0103 & -0.1289\times10^{-3}\ \text{m} & 16.3370\times10^{-3}\ \text{m} & 0.1929\times10^{-3}\ \text{m} \\ -68.4143\ \text{D} & -1.2012\ \text{D} & 0.9047 & -0.0103 & -0.0175 \\ -1.0994\ \text{D} & -61.7701\ \text{D} & -0.0103 & 0.8842 & 0.0084 \\ 0 & 0 & 0 & 0 & 1 \end{pmatrix}$$

and

$$\mathbf{T}_b=\begin{pmatrix} -0.1846 & -0.0139 & 16.3646\times10^{-3}\ \text{m} & -0.1324\times10^{-3}\ \text{m} & -0.3227\times10^{-3}\ \text{m} \\ -0.0125 & -0.0421 & -0.1322\times10^{-3}\ \text{m} & 16.1112\times10^{-3}\ \text{m} & 0.1974\times10^{-3}\ \text{m} \\ -71.2792\ \text{D} & -1.2564\ \text{D} & 0.9015 & -0.0107 & -0.0183 \\ -1.1461\ \text{D} & -64.3705\ \text{D} & -0.0107 & 0.8802 & 0.0086 \\ 0 & 0 & 0 & 0 & 1 \end{pmatrix},$$

where **B** and **e** are in metres and **C** is in dioptres.

Aperture-independent chromatic properties

For illustrative purposes, the calculation of chromatic difference in power and refractive compensation is:

$$\delta\mathbf{F}=\begin{pmatrix} -71.2792 & -1.2564 \\ -1.1461 & -64.3705 \end{pmatrix}-\begin{pmatrix} -68.4143 & -1.2012 \\ -1.0994 & -61.7701 \end{pmatrix}=\begin{pmatrix} 2.8649 & 0.0552 \\ 0.0468 & 2.6004 \end{pmatrix}\text{D}$$

and

$$\delta\mathbf{F}_0=\begin{pmatrix} -11.2891 & -0.8688 \\ -0.8688 & -2.6212 \end{pmatrix}-\begin{pmatrix} -8.9731 & -0.8092 \\ -0.8092 & -0.6380 \end{pmatrix}=\begin{pmatrix} -2.3160 & -0.0596 \\ -0.0596 & -1.9833 \end{pmatrix}\text{D},$$

from which it is clear that this is a myopic astigmatic eye.

Aperture-dependent chromatic properties

In order to obtain $\delta\mathbf{y}_R$, $\delta\mathbf{a}_R$, $\delta(\Delta\mathbf{y}_R)$, $\delta(\Delta\mathbf{a}_R)$, $\mathbf{M}_{yR}$ and $\mathbf{M}_{aR}$, we need the chromatic difference in coefficient matrices. The red and blue coefficient matrices are

$$\mathbf{V}_E^r=\begin{pmatrix} -0.1719 & -0.0148 & 17.0341\times10^{-3}\ \text{m} & -0.0903\times10^{-3}\ \text{m} & -0.3210\times10^{-3}\ \text{m} \\ -0.0139 & -0.0116 & -0.0923\times10^{-3}\ \text{m} & 16.3674\times10^{-3}\ \text{m} & 0.1928\times10^{-3}\ \text{m} \\ -59.3506\ \text{D} & -0.9477\ \text{D} & 0.8345 & -0.0053 & -0.0163 \\ -0.8961\ \text{D} & -52.0286\ \text{D} & -0.0054 & 0.7998 & 0.0091 \\ 0 & 0 & 0 & 0 & 1 \end{pmatrix}$$

and

$$\mathbf{V}_{\mathrm{E}}^{\mathrm{b}} = \begin{pmatrix} -0.2145 & -0.0154 & 16.9208\times10^{-3}\ \mathrm{m} & -0.0924\times10^{-3}\ \mathrm{m} & -0.3340\times10^{-3}\ \mathrm{m} \\ -0.0145 & -0.0475 & -0.0946\times10^{-3}\ \mathrm{m} & 16.2242\times10^{-3}\ \mathrm{m} & 0.1992\times10^{-3}\ \mathrm{m} \\ -61.5222\ \mathrm{D} & -0.9849\ \mathrm{D} & 0.8290 & -0.0054 & -0.0170 \\ -0.9291\ \mathrm{D} & -53.8848\ \mathrm{D} & -0.0055 & 0.7933 & 0.0094 \\ 0 & 0 & 0 & 0 & 1 \end{pmatrix},$$

with units given in metres (m) and dioptres (D).

References

1. Harris WF, Evans T. Chromatic aberration in heterocentric astigmatic systems including the eye. Optom Vis Sci. 2012;89:e37–e43 and appendix. https://doi.org/10.1097/OPX.0b013e31826c184d
2. Villegas ER, Carretero L, Fimia A. Le Grand eye for the study of ocular chromatic aberration. Ophthal Physiol Opt. 1996;16:528–531. https://doi.org/10.1016/0275-5408(96)00007-5